CHAPTER-5

SYNTHESIS OF GRAPHENE AND ITS APPLICATION IN DSSC FABRICATION

This chapter discusses characterization study of graphene synthesized by physical, chemical, and combined exfoliation synthesis route. This chapter shows application of graphene as counter electrode in DSSC fabrication. Use of synthesized graphene to increase conductivity of electrolyte is shown.

5.1 Synthesis of graphene

5.1.1 SEM-EDAX analysis

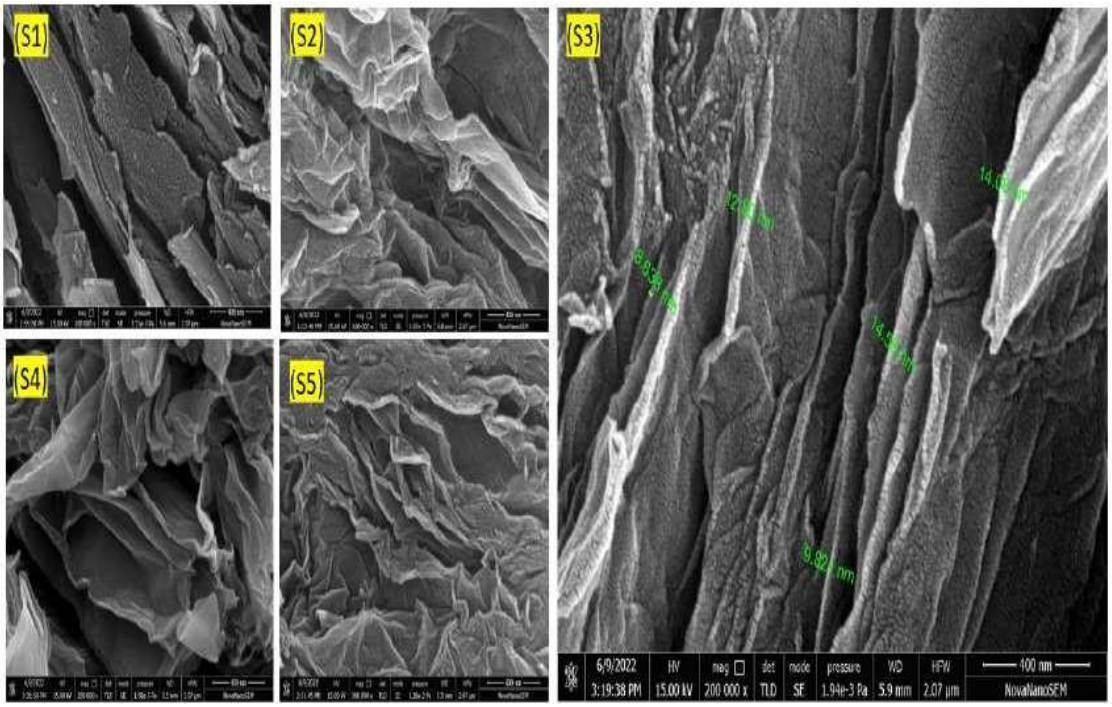

Fig. 35: HR-SEM images of graphene and RGO synthesized by various routes

Field Emission Scanning Electron Microscope (FESEM) analysis was used

to study the surface morphology of graphene. The top surface and cross- section view of Graphene has been shown in the Fig. 35 at 200X magnification. From the SEM images, it is evident that all samples have amultiple-layer structure, and it is possible to distinguish the edges ofindividual sheets from images. The thickness of layers of graphene (S2-S5) was found to be much larger than that of S1 graphene. The increase in the thickness is due to the introduction of oxygen-containing functional groupsduring the oxidation process and incomplete reduction. Samples S3, S4, and S5 showed more flaked and broken sheets. Flaked and broken sheets were formed due to a higher extent of physical and chemical exfoliation done in samples S3, S4, and S5.

Table 3: EDAX weight percent composition data of graphene samples

Element	**S1**	**S2**	**S3**	**S4**	**S5**
C	89.29%	51.03%	53.67%	56.50%	65.15%
O	10.71%	34.64%	31.83%	28.15%	22.57%
N	-	11.32%	13.09%	13.91%	7.85%
Mn	-	0.85%	0.55%	0.57%	1.45%
Traces	-	2.16%	0.86%	0.87%	2.98%
C/O Ratio	8.337	1.473	1.686	2.007	2.886

EDAX analysis:

The EDAX analysis suggests that S1 samples have the highest C/O ratio (Table 3) increases in reduced graphene oxide from sample S2

because it is produced by the liquid exfoliation method where no oxygen is incorporated for synthesis. It shows that by increasing exfoliation, the C/O to S5. Sample S5 has the highest C/O ratio in comparison to S2, S3, and S4 because a higher extent of exfoliation enhances the reduction of graphite oxide sheets. Exfoliation plays an important role in the efficient reduction of oxygenated carbon. A higher extent of exfoliation leads to better separation and segregation of sp^2 hybridized 2D hexagonal carbon sheet. In turn, the reducing agent gets to reach exfoliated oxygenated 2D hexagonal carbon sheets more efficiently. Thus, more oxygen is reduced. According to the extent of exfoliation, oxygen content decreases and carbon content increases in RGO samples. Also, none of the samples S2, S3, S4, and S5's C/O content ratio reaches S1. This confirms the incomplete reduction of samples.

5.1.2 XRD analysis

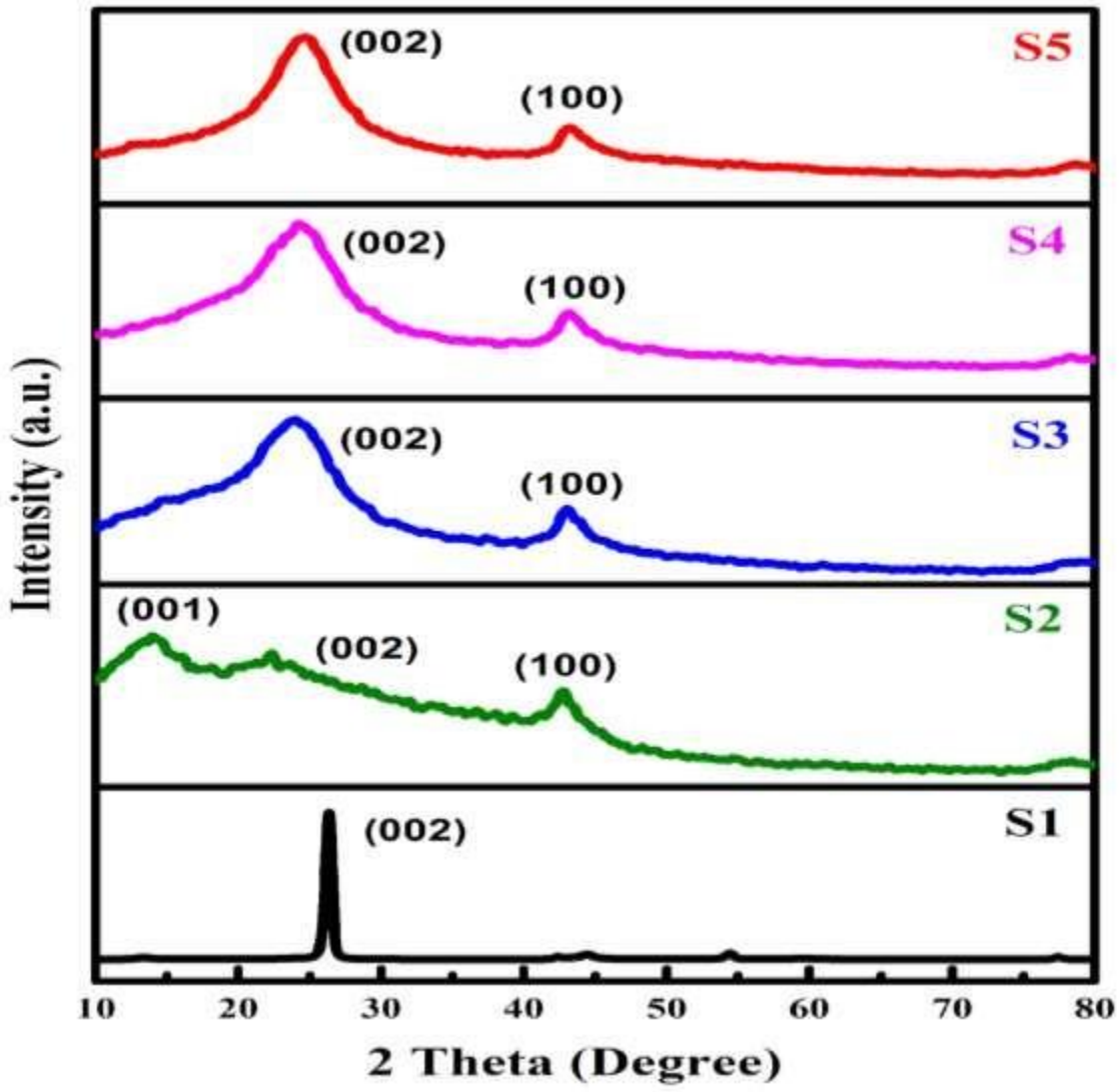

Fig.36: XRD plot of all synthesized graphene samples

The X-ray diffraction was done to observe the chemical composition of a material, its crystallinity, and phase. The XRD patterns of graphene nano-sheets synthesized from five different routes have been depicted in Fig.36. For S1 a sharp peak (002) at 26.36˚ is observed. This strong peak is characteristic of graphite and its crystalline nature. The value of d-spacing is calculated from Bragg's law which is 0.337 nm. For S1 the value of d-

spacing is very close to the thickness of the Graphene layer (0.335 nm). This confirms that exfoliation of graphite in NMP for sufficient time produces pure and good-quality graphene. For S2, at (001), (002), and (100) diffraction lines, small diffraction peaks at 14.2˚, 22.3˚, and 42.8˚ were observed respectively. The broad curve in the 14˚ to 28˚ 2θ region is indicative of the formation of an amorphous phase. The peak at 14.2˚ is indicative of the presence of various oxygen-containing functional groups. The d-spacing at 14.2˚ and 22.3˚ are 0.632 nm and 0.397 nm respectively, larger than the thickness of the Graphene Layer (0.335 nm). For the S2 sample, d-spacing at 14.2˚ is almost 2 times the thickness of the graphene layer due to the presence of oxygen-containing functional groups. This confirms the incomplete reduction of S2. The diffraction peaks of S3, S4, and S5 were observed at 24.02˚, 24.22˚, and 24.7˚ (002) diffraction lines, respectively. The d-spacing of S3, S4, and S5 at (002) diffraction lines are 0.370 nm, 0.367 nm, and 0.360 nm, which are slightly larger than the value of the thickness of the Graphene layer (0.335 nm). Interlayer spacing decreases with adding physical exfoliation steps from S3 to S5. The appearance of the (002) diffraction line in the XRD pattern shows that S3, S4, and S5 are ordered crystal structures. The absence of a peak at 2θ = 26.36˚ degrees for S3, S4, and S5 indicates the complete conversion of graphite to graphite oxide and can be related to the efficiency of the Oxidation process. The absence of a peak at 14.20˚ degrees for S3, S4, and

S5 indicates the almost complete reduction of graphene oxide and can be related to the efficiency of the reduction process. The peak present at 2θ = 43˚in samples S2, S3, S4, and S5 is due to defects in RGO [131] or the presence of MnO_2 in samples. Interlayer spacing (d), average crystallite width (D), in-plane crystallite size (L), and number of layers (n) are some of the parameters that were calculated from the equations below [132] and are listed in the table 4.

$$d = \frac{\lambda}{2*sin\theta} \text{.....(i)}$$

$$D = \frac{k*\lambda}{FWHM*cos\theta} \text{. .....(ii)}$$

$$n = \left(\frac{D}{d}\right) + 1 \text{. .....(iii)}$$

$$L = \frac{1.84*\lambda}{FWHM*cos\theta} \text{. .....(iv)}$$

where d = interlayer spacing, 2θ= diffraction angle, λ = X-ray wavelength, k = 0.9 (constant, which depends on crystallite shape), FWHM = full width at half maximum, D = average crystallite width, L = in-plane crystallite size, and n = Number of layers per domain.

Table 4: Different parameters of all samples from XRD data

Sample	2θ(˚C)	β (FWHM)	d (nm)	D (nm)	n
S1	26.36	0.55	0.337	14.8	44.9
S2	14.20	4.00	0.632	3.0	8.2
S3	24.02	7.70	0.370	2.6	3.8
S4	24.22	7.20	0.367	2.7	4.1
S5	24.70	6.05	0.360	2.8	4.7

Average crystallite width and in-plane crystallite sizes are less for combined methods than individual exfoliation methods. Also, no. of layers per domain is less for combined exfoliation methods than individual exfoliation methods.

5.1.3 Raman spectral analysis

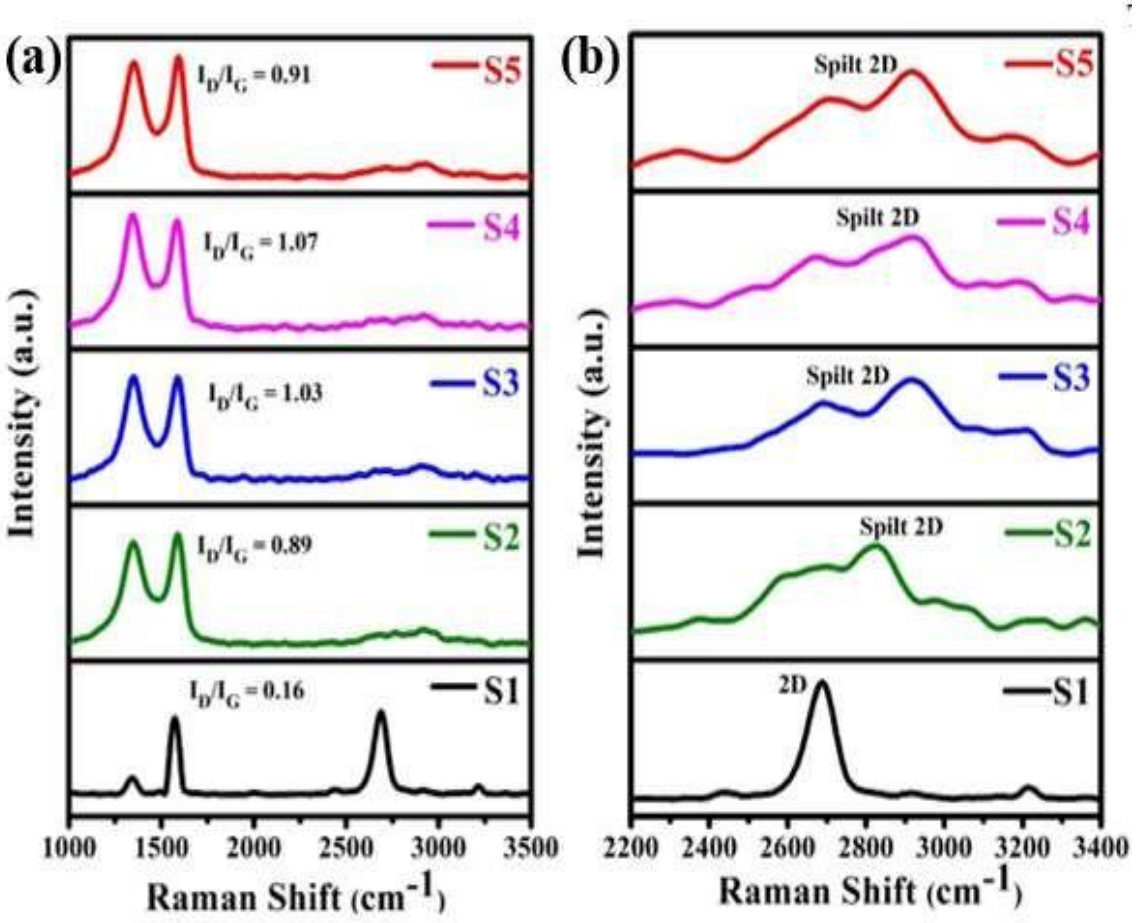

Fig.37: Raman spectra of synthesized graphene and RGO samples by various routes (a) showing D, G, and 2D peak and (b) showing 2D peak

Raman spectroscopy is used to examine carbon containing nano-materials. The Fig.37 shows the Raman spectra of produced graphene. The E_{2g} phonon of the sp^2 C atoms is represented by the G band at 1605 cm^{-1} in the usual Raman spectra of graphene. The G-band is associated with graphitic carbons, while the breathing mode of the k-point phonons of the A_{1g} symmetry is represented by the D band at 1353 cm^{-1}. The D-band is related to structural defects or partially disordered graphitic domains. Defects such as vacancies, grain boundaries, and amorphous carbon species, cause the appearance of the D band in the Raman Spectra of any sample. The graphene's quality is indicated by the intensity ratio of these two bands, I_D/I_G. Raman spectral studies demonstrate that S2, S3, S4, and S5 products are structurally the same while S1 is different due to using chemical and physical exfoliation synthesis routes. The D-bands in S2, S3, S4, and S5 sample spectra are strong, confirming the lattice distortions of graphene basal planes. In the Raman spectra, an obvious D band peak appears which is probably due to the presence of sp^3 defects formed by unavoidable oxidation in the electrochemical exfoliation process. A strong D peak is usually present in graphene samples which are synthesized by chemical exfoliation route. A weak D peak is present in the S1 sample because S1 is synthesized by the liquid exfoliation route, which is free from structural defects. The I_D/I_G ratio is 0.16, 0.89, 1.03, 1.07, and 0.91 for samples S1,

S2, S3, S4 and S5 respectively. The low I_D/I_G ratio for sample S1 is an indication of a strong G peak and a very weak D peak. This is an indication of a structure with better graphitization and fewer defects. Increased I_D/I_G ratio was observed for samples S2, S3, S4, and S5 due appearance of strong equal intensities of D and G peaks. I_D/I_G ratio increased from sample S2 to S4 slightly and then a slight decrease in value was observed for S5. This is because of an increase in defects for samples S2, S3, and S4. A slight restoration of the sp^2 hexagonal structure for sample S5. The lower intensity ratio (I_D/I_G) of the D band and G band imply a decrease in the average size of the sp^2 domains and a partially ordered crystal structure. Two other bands were observed at 2700^{-1} and 2900 cm^{-1}. For monolayer graphene, there is a sharp peak at 2700 cm^{-1}. The band at 2700 cm^{-1} is known as the 2D band, which is an indicator of the number of graphene layers. The I_{2D}/I_G ratio indicates the thickness of the exfoliated sheet as well as the number of sheets attached. A sharp 2D peak is observed for theS1 sample at 2684 cm^{-1} and the I_{2D}/I_G ratio is 0.70. This indicates that 2D sp^2 hexagonal graphene sheets were exfoliated and segregated well. Only a few graphene layers are present in sample S1. Broad, weak, and spilled 2D peaks were observed for samples S3, S4, and S5. This indicates that many 2D RGO sheets were stacked together and not exfoliated well. Also,the quality of RGO sheets was poor due to many layers stacking and

incomplete reduction. 2D peaks spilt in $2D_A$, $2D_B$ and $2D_C$ around 2684 cm^{-1}, 2770 cm^{-1}, 2870 cm^{-1} respectively for sample S2, S3, S4 and S5. The I_{2D}/I_G are 0.13, 0.16, 0.12, and 0.11 for sample S2, S3, S4 and S5 respectively. The I_{2D}/I_G ratio for sample S3 is highest among samples that were produced by chemical exfoliation i.e. oxidation-reduction synthesis route. This confirms that exfoliation before and during reduction plays a significant role in improving the quality of RGO sheets. Another band, known as the S3 band (2900 cm^{-1}), is a second-order peak derived from the D–G peak combination. S3 band appearance indicates $–CH_2$ vibrations. The intensity ratio of S3 relative to 2D is proportional to the reduction in defects. This reduction is accompanied by a lower oxygen content in graphene. The I_{S3}/I_{2D} ratio is 1.1, 0.98, 1.15, and 1.12 for samples S2, S3, S4 and S5 respectively. The intensities of both peaks increased in the case of graphene, indicating better graphitization. Here, we observed that the $IS3/I_{2D}$ ratio for samples S2, S3, S4 and S5 are ~ 1. Thus, restoration of graphitic structure came out for all RGO samples. The overtone of the D line, the 2D line, is located at 2700 cm^{-1}, while the 2G line (the overtone of the G line) is around 3200 cm^{-1}. As sample S1 is chemically different from the rest, poor peaks were observed at 2900 cm^{-1} and 3200 cm^{-1} as compared to 2D peaks. The peak at 3200 cm^{-1} indicates vibrational stretching of the -OH bond. This confirms the incomplete reduction of oxidized graphene

oxide. The intensity ratio I_{S3}/I_{2G} indicates the content ratio of $–CH_2$ to –OH group. The I_{S3}/I_{2G} ratios are 2.8, 1.5, 2.0, and 3.4 for samples S2, S3, S4 and S5 respectively. This is in accordance with EDAX analysis, where the maximum extent of reduction was observed in sample S5. Also, a similar increasing trend for C/O content was observed in EDAX analysis for samples S3, S4, and S5. Thus, it is again confirmed from Raman spectral analysis that exfoliation plays a significant role in the efficient reduction of GO. Various peak ratios are listed in the table 5.

Table 5: I_D/I_G, I_{2D}/I_G, I_{S3}/I_{2D} and I_{S3}/I_{2G} ratio values of all samples.

Sample	**I_D/I_G**	**I_{2D}/I_G**	**I_{S3}/I_{2D}**	**I_{S3}/I_{2G}**
S1	0.16	-	-	-
S2	0.89	0.13	1.10	2.3
S3	1.03	0.16	0.98	1.5
S4	1.07	0.12	1.15	2.0
S5	0.91	0.11	1.12	3.4

5.1.4 HRTEM analysis

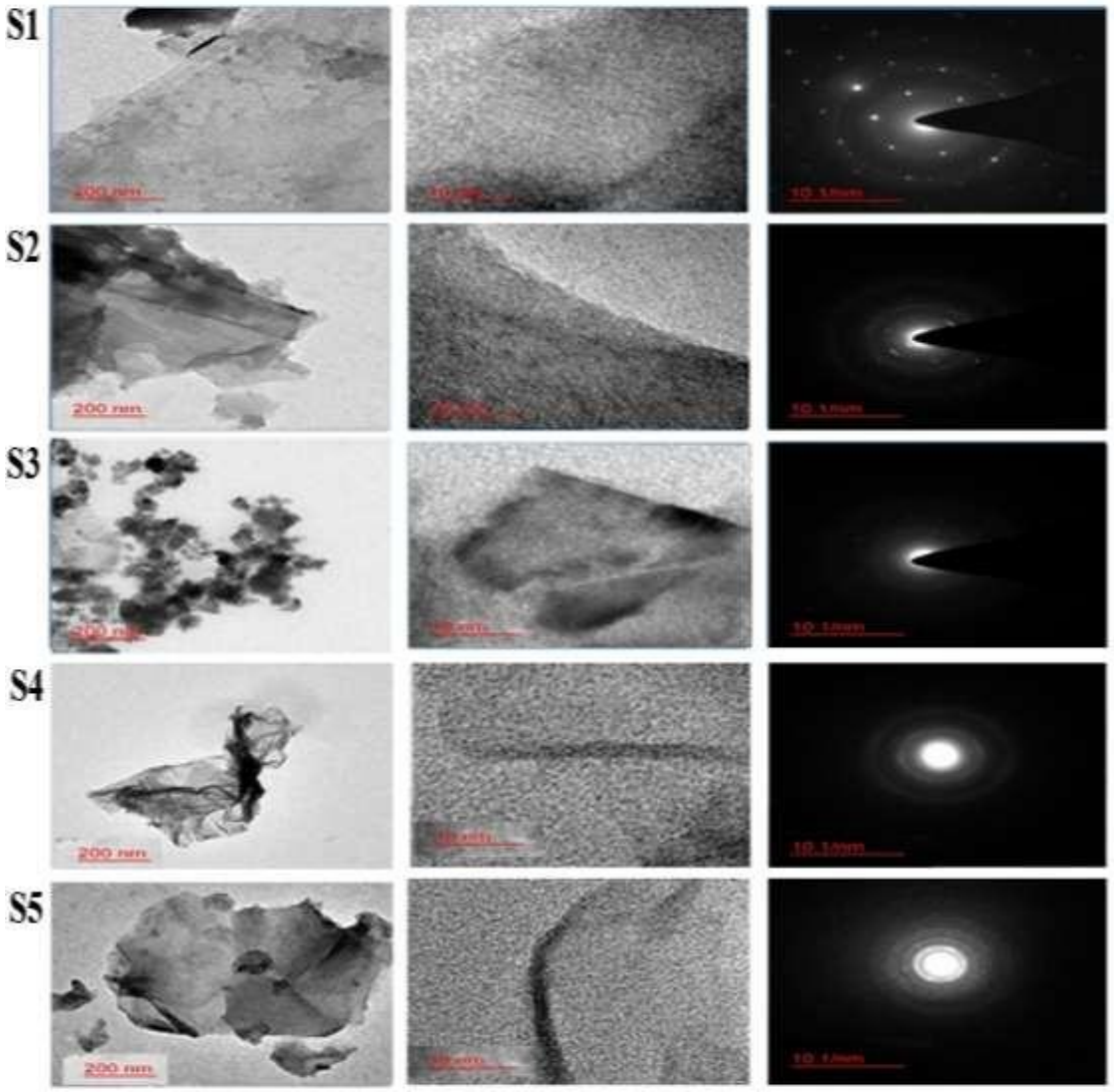

Fig. 38: TEM images of all samples S1, S2, S3, S4 & S5, their TEM micrographs showing lattice fringes and their corresponding SAED pattern.

Fig.38. shows lower magnification HRTEM images, HRTEM micrograph showing lattice fringes, and SAED Pattern of samples S1, S2, S3, S4, and S5. Lattice fringe gives additional information about interplanar distance. The SAED pattern gives an idea of the crystallographic structure of the

graphene sheets. The TEM image of S1 and S2 showed that many layers and some layers are stacked together. The TEM image of S2 showed some layers are attached. The TEM images of S3, S4, and S5 showed very few broken sheets attached. TEM images of all samples are reconfirming findings of XRD data, where no. of layers per domain for S1, S2, S3, S4, and S5 were ~44, ~8. ~3, ~4 and ~4, respectively. TEM micrographs showing lattice fringes of S1, S2, S3, S4, and S5 gave inter-layer d-spacing of 0.35 nm, 0.774 nm, 0.433 nm, 0.357 nm, and 0.333 nm respectively. Inter-layer d-spacing from HRTEM micrographs for all samples is in a similar trend with XRD data. SAED pattern of S1 confirmed the sp^2 hybridized hexagonal structure of exfoliated graphene sheets. The SAED pattern of S2, S3, S4, and S5 showed a distorted hexagonal structure of RGO sheets. The SAED pattern further confirmed the disordered nature of the RGO nanosheets. The SAED pattern of RGO shows only diffraction rings and the diffraction dots are undifferentiated from rings indicating that the RGO flakes are amorphous. This result is consistent with XRD analysis. Some more HRTEM images at lower and higher magnification along with interlayer d-spacing calculation images are attached in the supplementary data file.

5.1.5 EIS Study

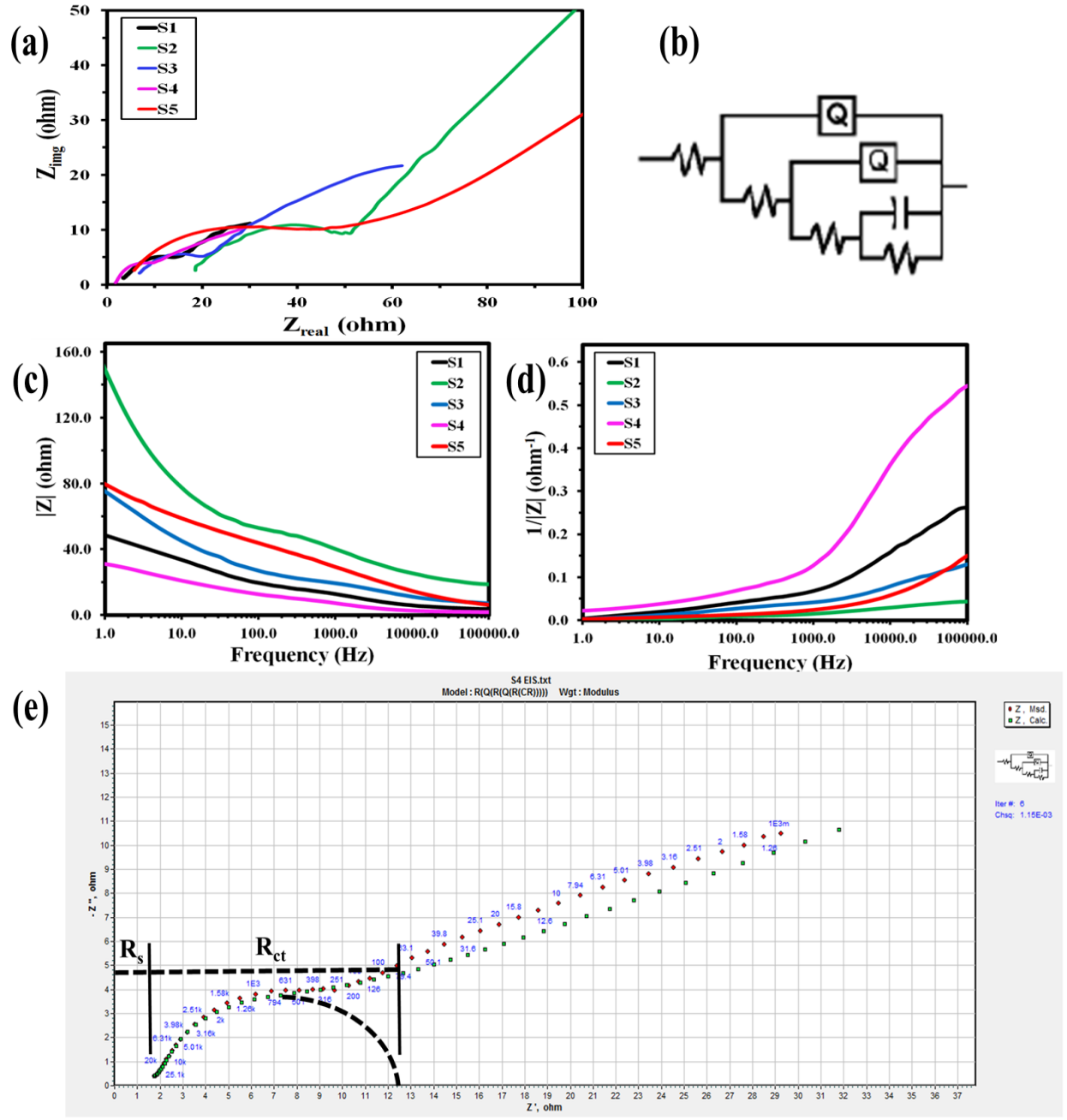

Fig 39. (a) Nyquist plots all samples, (b) Equivalent circuit of S4, (c) |Z| vs Frequency, (d) |Y| vs Frequency of all synthesized samples, and (e) curve fit of S4.

Nyquist plot of all samples is shown in Fig.39. a. Equivalent series resistance (Rs), and resistance resulting from charge-transfer (Rct) of all samples are calculated from the Nyquist plot and are listed in Table 6. During the plotting of a quasi-semicircle, the x-axis intercept is noted as Rs, and the semicircle diameter is defined as Rct. Rs values obtained for S1, S2, S3, S4, and S5 are 2.1Ω, 15.6 Ω, 4.4 Ω, 1.3 Ω and 3.9 Ω, respectively. Sample S4 showed the lowest value of Rs which was mainly because of lower intrinsic resistance. Rs value of only chemically exfoliated sample S2 is highest, showing higher intrinsic resistance. Rct values obtained of S1, S2, S3, S4, and S5 are 19.7 Ω, 40.4 Ω, 23.1 Ω, 12.2Ω, and 45.8 Ω, respectively. The Rct value of S4 is the lowest indicating the lowest percentage of oxygen present in the sample. The Rct value of S1 is also low because of using a physical exfoliation method. A decrement in Rct value is observed when physical exfoliation is introduced at various steps in the chemical exfoliation method for S2, S3, and S4. In Figure 39.a. graphene sample 4 (S4) showed the smallest semi-circle in the low frequency region among all which stands for the highest conductivity while S2 and S5 show the lowest conductivity. The equivalent circuit for S4 is shown in Fig 39.b. Rs and Rct values of S4 are shown in Fig. 39.e. Total resistance, Z vs Frequency plot is shown in Fig 39.c. S4 showed a lower value of Z in all frequency ranges. Also, a lower value of Z is observed at higher frequency regions. 1/Z vs Frequency plot is shown in

Fig 39.d. S4 showed the highest conductance among all samples in the whole frequency region. Also increased conductance is observed for all samples as frequency increases. Graphene synthesized from combined exfoliation methods is more conductive than graphene synthesized via physical or chemical exfoliation methods.

Table 6: Different resistance values of different samples

Sample	R_s (Ω)	R_{ct} (Ω)
S1	2.1	19.7
S2	15.6	40.4
S3	4.4	23.1
S4	1.3	12.2
S5	3.9	45.8

5.1.6 Particle size distribution study

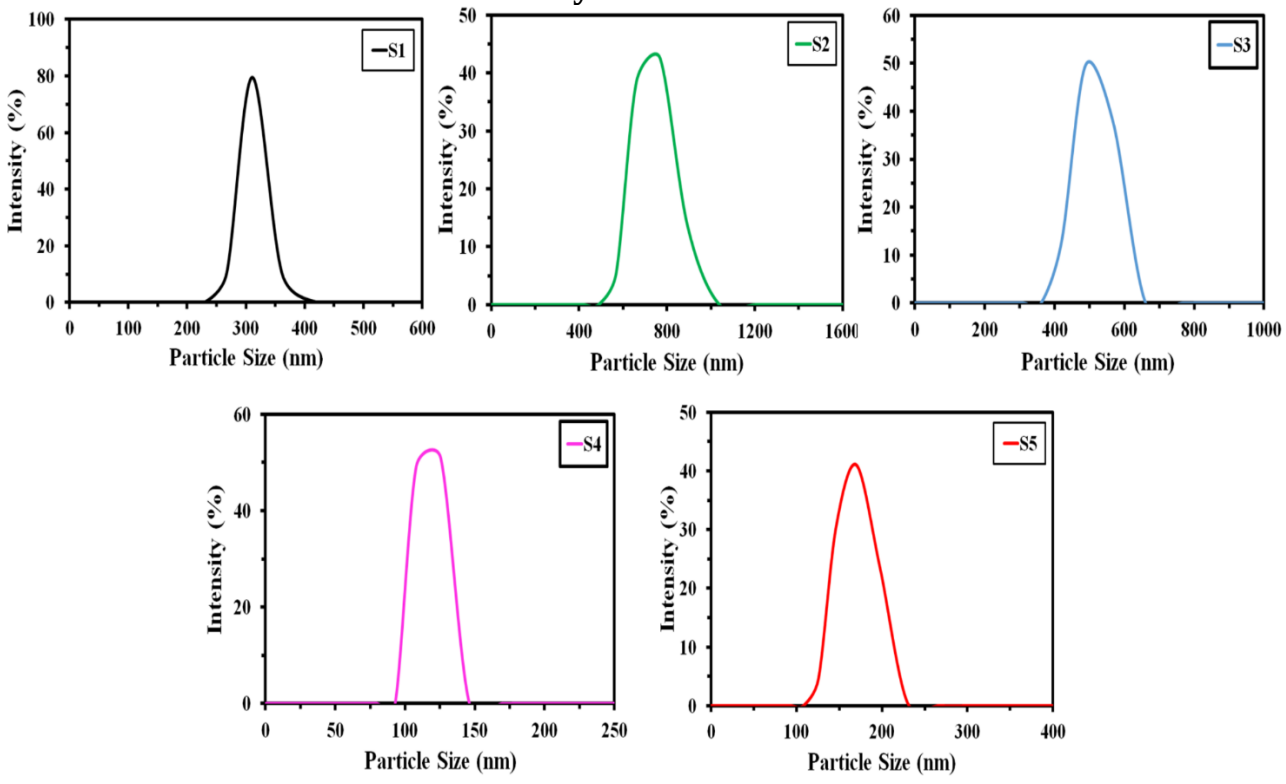

Fig.40: Particle Size distribution of all synthesized graphene samples

The particle size distribution of various samples is shown in Fig.40. For S1, S2, S3, S4, and S5, the particle sizes were found to be 311.4 nm, 733.4 nm, 509.8 nm, 112 nm, and 167.5 nm, respectively. The polydispersity index (PDI) of S1, S2, S3, S4, and S5 were 0.68, 0.28, 0.58, 1.47, and 0.36 (Table 7). Smaller values of PDI showed uniformity and less agglomeration in all samples. According to the findings, S4 has a smaller average particle size than the other samples. Smaller average particle sizes have been observed due to combining both physical and chemical exfoliation than implying any single exfoliation technique.

Table 7: Average particle size and polydispersity index of all samples

Sample	Average Particle Size (nm)	Polydispersity Index (PDI)
S1	311.4	0.68
S2	733.4	0.28
S3	509.8	0.58
S4	112.0	1.47
S5	167.5	0.36

5.1.7 UV-Vis absorbance study

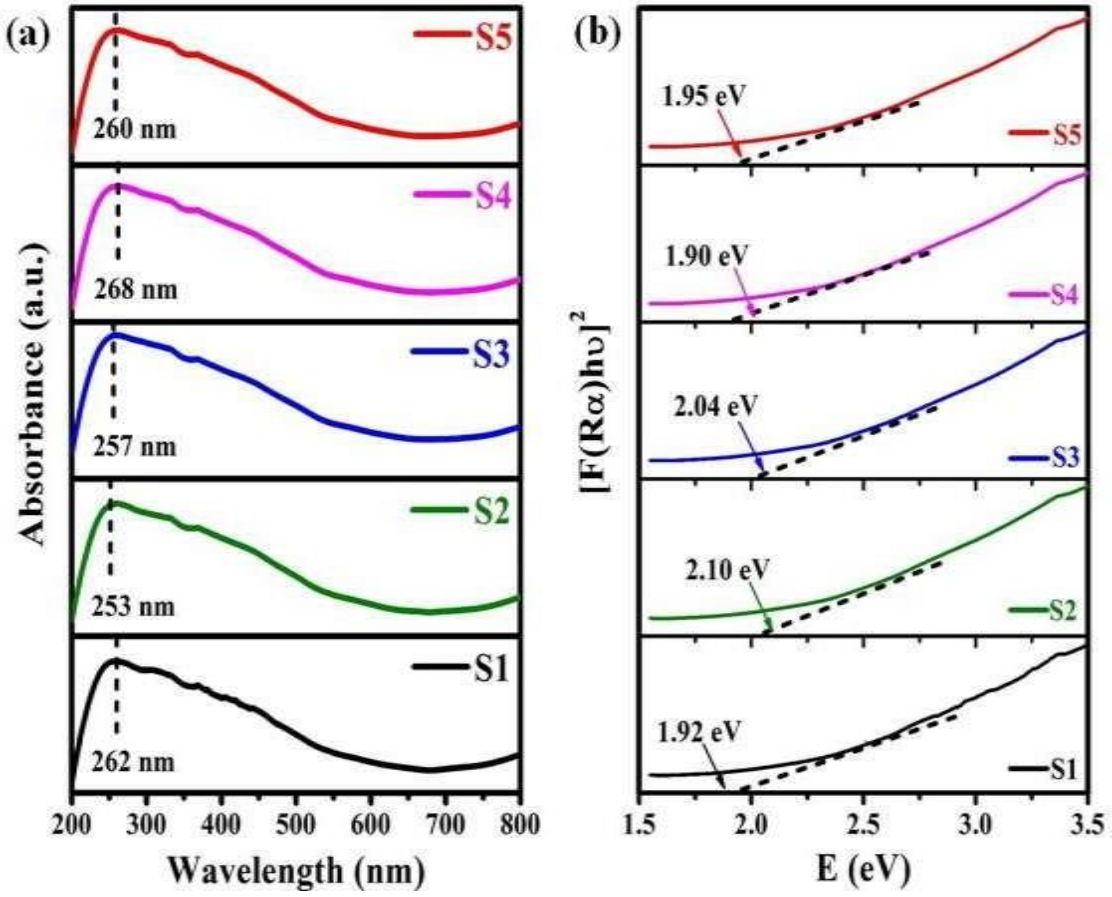

Fig.41: (a) UV-Vis Spectra and (b) Band Gap of all graphene samples

Maximum absorbance of S1, S2, S3, S4, and S5 are observed at 262 nm, 253 nm, 257 nm, 268 nm and 260 nm (Table 8, Fig. 41) respectively. λmax of S2 is the lowest among all due presence of more π–π bonds. The presence of more π–π bonds implies incomplete reduction and higher oxygen content. Hence bandgap of S2 (2.10 eV) is the highest among all. Higher oxygen content makes the RGO sample more resistive. Similarly, λmax of S4 is the highest among all due presence of more σ bonds. The

presence of more σ bonds implies better reduction and lower oxygen content. Therefore, bandgap of S4 (1.90 eV) is the lowest among all, making it the most conductive. λmax of S1 is lower than λmax of S4 because S4 is both physically and chemically exfoliated, while S1 is only physically exfoliated. Even though oxygen is added during the oxidation process to S4 (which also exfoliates S4 by adding oxygen groups between layers), due to physical exfoliation at each step more σ bonds are present in S4. Also, due to exfoliation at each step, the reduction process is efficient in S4, which further increases σ bonds in S4. Therefore, band gap of S1 (1.92 eV) is slightly higher than S4. S1 is less conductive than S4 because it is only physically exfoliated. Similarly, λmax of S3 is higher than S2 due to increased exfoliation than S2, which in turn ensures better reduction in S3 than S2. Hence oxygen content also increases in S3. Also, band gap of S3 (2.04 eV) is lower than S2, making it more conductive than S2. λmax of S5 is lower than S4 even though it has the lowest oxygen content. This is due to intense exfoliation in S5, its sheets are broken. Hence, lesser σ bonds are present in S5. Therefore, bandgap of S5 (1.95 eV) is higher than S4. However, S5 is more resistant than S4 even when it has less oxygen content than S4.

Table 8: λmax and band gap of all samples

Sample	λmax (nm)	Band Gap (eV)
S1	262	1.92
S2	253	2.10
S3	257	2.04
S4	268	1.90
S5	260	1.95

5.2 Application of graphene as counter electrode

Counter electrodes with graphene S1 solution and S4 solution were prepared and DSSCs were fabricated using S1 and S4 counter electrodes labeled as S1 DSSC and S4 DSSC, respectively. Jsc, Voc, FF, and η data of standard DSSC with Pt as a counter electrode labeled as Pt DSSC were compared with S1 and S4 DSSC in the table. JV plots of Pt DSSC, S1 DSSC, and S4 DSSC were plotted in Fig.42. This work aimed to replace expensive Pt counter electrodes with much cheaper graphene counter electrodes. Jsc of S4 DSSC (8.5 mA/cm^2) is higher than Jsc (8.2 mA/cm^2) of Pt DSSC. This is due to the low charge transfer resistance of 12.2Ω offered by S4 counter electrodes. S4 counter electrodes offer very low resistance to electron flow, Hence the rate of flow of electrons is higher in S4 DSSC. Jsc (7.9 mA/cm^2) is very close to Jsc of Pt DSSC due to S1 charge transfer resistance 19.7 Ω is very low. S1 also offers very low

resistance to electron transfer. Hence the rate of electron transfer in S1 DSSC is comparable to Pt DSSC. Voc of Pt DSSC, S1 DSSC, and S4 DSSC are 0.63 V, 0.62V and 0.64 V, respectively. Voc graphene DSSC isvery close to Pt DSSC. This is due to the very low band gap of 1.90 eV,

1.92 eV is offered by S1 and S4 counter electrodes, respectively in comparison to Pt counter electrodes (~1.5 eV). The fill factor of Pt DSSC, S1 DSSC, and S4 are close to one another. The efficiency of Pt DSSC, S1 DSSC, and S4 DSSC are 3.2 %, 3.1 % and 3.4 % (Table 9) respectively.S4 DSSC gave higher efficiency than Pt DSSC due to low charge transfer resistance and higher electro-catalytic activity towards I_3^-. Graphene (S4) synthesized via the chemical exfoliation route showed higher efficiency due to oxygen functional group defects, which are active sites for I_3^-ions to gain electrons and reduce to I^-. The reduction reaction of $I_3^-$to I^- is a favorable reaction for higher efficiency. Graphene S1 synthesized with physical exfoliation does not have these oxygen functional group defects. Therefore, lower efficiency was shown in S1 DSSC. Therefore, graphene can be used as a cheaper and better replacement as a counter electrode material in DSSC. Only adhesion of graphene needs to be taken care of by adding conductive binders like nafion and PEDOT/PSS to its solution.

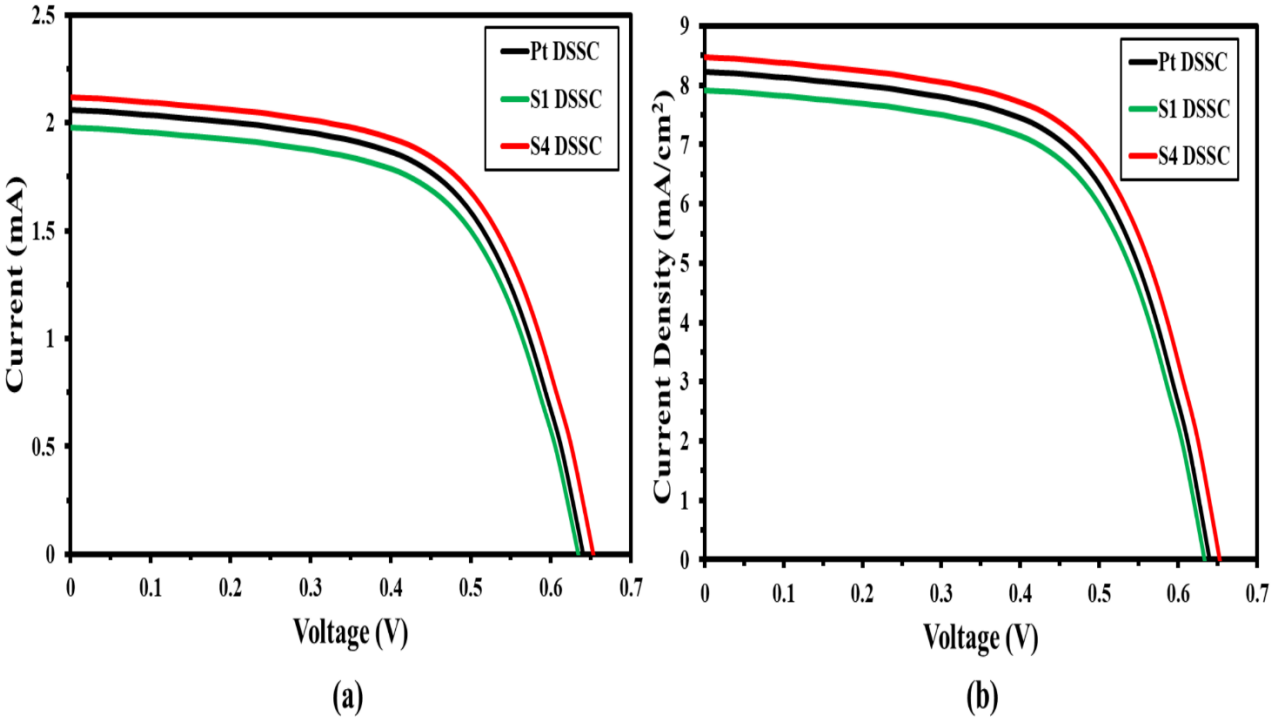

Fig.42: (a) IV & JV plot of DSSC fabricated using Pt, graphene S1, and graphene S4 as counter electrodes

Table 9: Jsc, Voc, FF, and η of DSSC fabricated using Pt, S1, and S4 as counter-electrode

Counter Electrolyte Material	Jsc (mA/cm^2)	Voc (V)	FF	η
Pt DSSC	8.2	0.63	0.62	3.2
S1 DSSC	7.9	0.62	0.63	3.1
S4 DSSC	8.5	0.64	0.62	3.4

5.3 Application of reduced graphene in liquid electrolyte of DSSC

5.3.1 Conductivity of liquid electrolytes

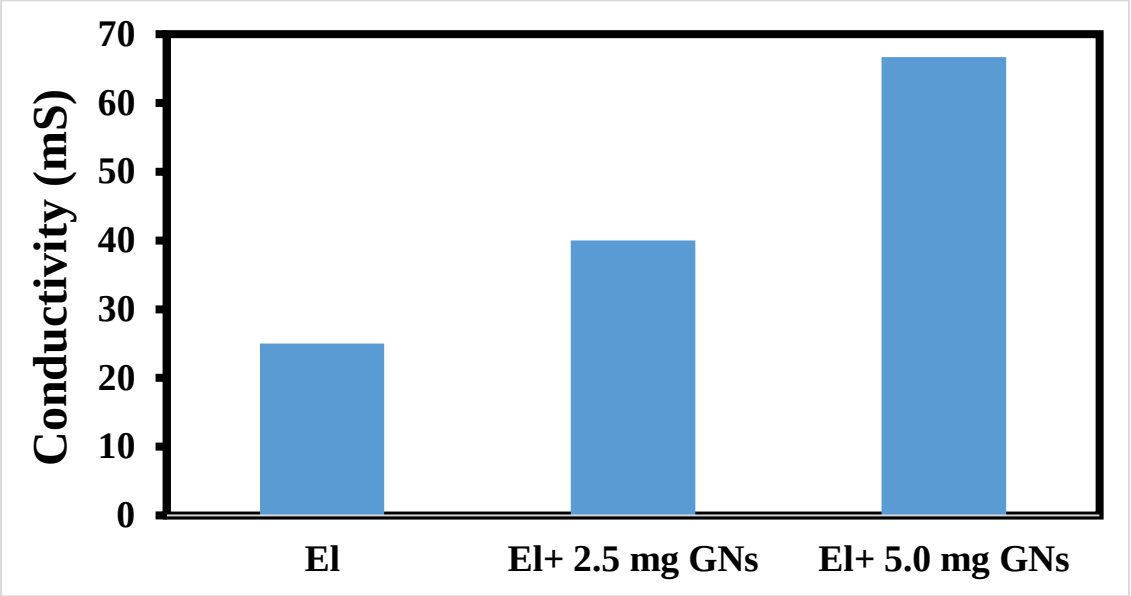

Fig. 43: Pictures of liquid electrolyte with graphene conc. (a) 0 mg/ml, (b) 2.5 mg/ml & (c) 5.0 mg/ ml

Conductivity of electrolyte increased as graphene sample is added to electrolyte. Electrolyte conductivity increases to 40 mS and 66.7 mS from 25 mS, if 2.5 mg and 5.0 mg of graphene is added to 1 ml of liquid electrolyte, respectively [144].

5.3.2 J-V characteristic study of graphene liquid electrolyte

RGO S4 was added to the liquid electrolyte in 0, 2.5 mg/ml, and 5.0 mg/ml concentration to prepare RGO S4 liquid electrolyte. These electrolytes were then used to fabricate DSSC labeled as 0 S4 DSSC, 2.5 S4 DSSC,

and 5.0 S4 DSSC. JV plots of these DSSCs are shown in Fig 43. and results are listed in the table 10. S4 graphene was selected out of all S1, S2, S3, S4, and S4 graphene due to the very low charge transfer resistance offered by it (discussed in detail in section 5.1.5). Also as discussed in section 5.2, the efficiency of the S4 counter electrode DSSC was even higher than the Pt counter electrode. The addition of S4 RGO increases the conductivity of the liquid, thus reducing charge transfer resistance. Hence increase in efficiency, Jsc, and Voc was observed for 2.5 S4 DSSC. Oxygen functional group defects present in S4 are active sites for I_3^-ions. Active sites of S4 increase the rate of reduction reaction of I_3^-ions to I^- ions in the electrolyte itself. Therefore, the overall rate of electron transfer increases in 2.5 S4 DSSC. Hence an increased value of current, voltage, and efficiency is observed.

Jsc (10.9 mA/cm^2) is higher for 2.5 DSSC than Jsc (8.2 mA/cm^2) of 0 S4 DSSC. This is due to the increased conductivity of the electrolyte and increased charge transfer resistance. Voc of 2.5 S4 DSSC (0.61 V) is close to Voc of 0 S4 DSSC (0.63 V) as Voc is mainly attributed to the number of electrons generated, which is not affected by the increasing conductivity of the electrolyte. However, the fill factor of 2.5 S4 DSSC (0.55) is lower than 0 S4 DSSC because of the graphene nanosheets present in electrolyte

deposits to the anode surface. 2.5 S4 DSSC showed the highest efficiency of 3.7 % than 0 S4 DSSC with 3.2 % efficiency due to increased rate offlow of electrons. Adding graphene to the electrolyte is favorable to only up to optimum conc. Adding more S4 graphene will not help in further enhancing the Jsc of DSSC as is observed in 5.0 S4 DSSC. Increased Jsc (11.6 mA/cm^2) of 5.0 S4 DSSC than 1.1 S4 DSSC due to higher conductivity of electrolyte will not ensure further enhancement in efficiency of 5.0 S4 DSSC. FF greatly reduces even though an increase in Jsc and Voc values of 5.0 S4 DSSC is observed. This is because graphene nanosheets in higher amounts will settle to the anode surface, thus reducing the fill factor. 3.5 % efficiency was observed for 5.0 S4 DSSC which is lower than the efficiency of 2.5 S4 DSSC. Therefore, adding graphene to electrolyte increases its efficiency by 15.6 % if used in optimum conc.

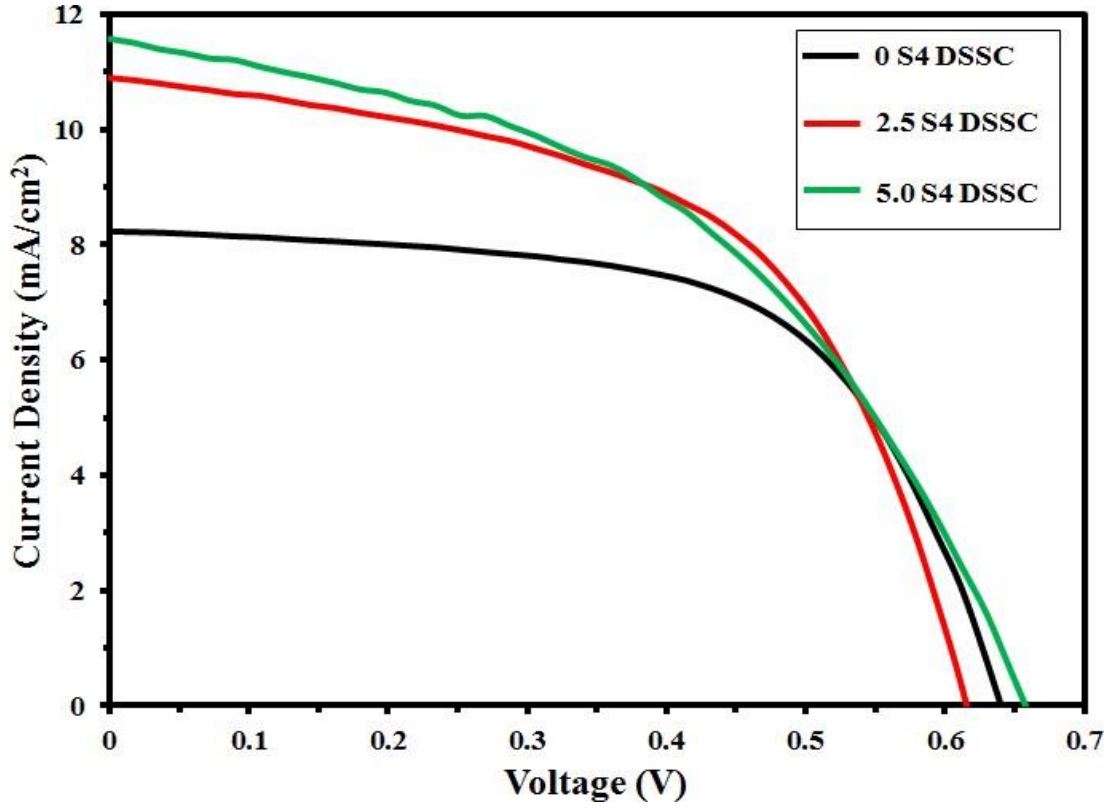

Fig.44: JV plot of DSSC fabricated using 0, 2.5 mg/ ml, 5.0 mg/ml S4 RGO in liquid electrolyte

Table 10: Jsc, Voc, FF, and η of DSSC fabricated using 0, 2.5 mg/ml, 5.0 mg/ml S4 RGO in liquid electrolyte

RGO (S4) in Electrolyte	Jsc (mA/cm^2)	Voc (V)	FF	η (%)
0 S4 DSSC	8.2	0.63	0.62	3.2
2.5 S4 DSSC	10.9	0.61	0.55	3.7
5.0 S4 DSSC	11.6	0.65	0.47	3.5

5.4 Conclusions

Varieties of graphene were synthesized. S1 was synthesized via physical exfoliation method using bath and probe sonication in NMP solvent. S2 was synthesized via chemical exfoliation methods using oxidation-reduction techniques. The physical exfoliation step was added before and during the reduction in the chemical exfoliation method to synthesize S3. Similarly, a physical exfoliation step was added during oxidation and before oxidation to synthesize S4 and S5, respectively. SEM images showed a few layers attached to each sample. S5 with a 2.886, C/O ratio showed that oxygen content decreased as more exfoliation steps were introduced. This result was further confirmed by Raman Characterization where the I_{S3}/I_{2G} ratio was 3.4, the highest among all. S3 synthesized via combined exfoliation method 3 number of layers per domain. This result was also confirmed by Raman Characterization where I_{2D}/I_G ratio was 0.16 highest among all. Graphene synthesized via combined exfoliation method showed low inter-layer d-spacing i.e. 0.370 nm, smallest average crystallite width of 2.6 nm, and smallest in-plane crystallite size of 2.2 nm for S3. Interlayer d-spacing values of S1, S2, S3, S4, and S5 from HRTEM fringe images were 0.35 nm, 0.774 nm, 0.433 nm, 0.357 nm and 0.333 nm respectively. A similar trend of inter-layer d-spacing was found in XRD data. TEM images also reconfirmed XRD data for the number of layers.

Particle size distribution was uniform with low PDI values for all samples. S4 showed the lowest average particle size of 112 nm with 1.47 PDI. S4 with the lowest value of Rs i.e. 1.3 Ω and Rct i.e. 12.2 Ω is the most conductive graphene, which was synthesized via the combined exfoliation method. UV plot and data further confirmed EIS study findings. The λmax of S4 is 268 nm (band gap = 1.90 e V), which is at a higher wavelength among all showing a greater number of σ bonds and lower oxygen content. The combined exfoliation method is better at producing good quality graphene than individual physical or chemical exfoliation methods. Also, Physical exfoliation added during oxidation, before reduction, and during the reduction step in the chemical exfoliation method to combine these two exfoliation methods are crucial steps in producing good quality graphene. S4 DSSC gave higher efficiency than Pt DSSC due low charge transfer resistance and higher electro-catalytic activity towards I_3^-. Graphene (S4) synthesized via chemical exfoliation route showed higher efficiency due oxygen functional group defects, which are active sites for I_3^- ions to gain electron and reduce to I^-. Graphene S1 synthesized with physical exfoliation do not have this oxygen functional group defect. Therefore, lower efficiency was shown in S1 DSSC.

Oxygen functional group defects present in S4 is active site for I_3^- ions. Active sites of S4 increase rate of reduction reaction of I_3^- ions to I^- ions in electrolyte itself. 2.5 S4 DSSC showed highest efficiency of 3.7 % than 0 S4 DSSC with 3.2 % efficiency due to increased rate of flow of electron.FF greatly reduces even though increase in Jsc and Voc values of 5.0 S4 DSSC is observed. This is due graphene nanosheets in higher amount willsettle to anode surface, thus reduces fill factor.